

## Ultrafast heating and switching of a semiconductor optical amplifier using half-cycle terahertz pulses

S. Hughes\* and D. S. Citrin

*Semiconductor Optics Theory Group, Department of Physics and Materials Research Center, Washington State University, Pullman, Washington 99164-2814*

(Received 29 May 1998)

Carrier heating of a semiconductor optical amplifier (SOA) using half-cycle terahertz pulses is investigated. For reasonable parameters, the electron-hole plasma temperature can be increased substantially. The subsequent change in the refractive index and gain profile of the SOA is predicted to be large enough to form the basis of a very efficient ultrahigh-speed optical switch. [S0163-1829(98)50248-2]

It is well known that the interaction of an intense optical pulse with a semiconductor optical amplifier (SOA) can lead to a significant heating of the electron-hole (e-h) plasma.<sup>1</sup> Recently it has been experimentally demonstrated that the optical perturbation of a semiconductor laser may turn the laser off on ultrafast timescales.<sup>2</sup> Ultrafast changes in the refractive index around the band edge have also been shown using semiconductor laser amplifiers.<sup>3</sup> This heating approach shows considerable promise for ultrahigh-speed modulation of SOA's since it may be possible to have large fast optical nonlinearities with gain rather than loss, and the switching figures-of-merit can be enormous. Additionally, semiconductor devices are particularly attractive for switching because a reliable materials industry has already been built around them. Unfortunately, for large-intensity optical control pulses, difficulties arise due to a net change in carrier density.

Turning now to practicalities, the next generation of broad-bandwidth optical communication networks with data rates of 100 Gbit/s and more will probably require ultrafast switching in simple pipeline processing architectures (i.e., not multiplexed) for some applications (for a review, see Ref. 4). Two of the most successful approaches so far—by exploiting an intensity-dependent refractive index—are based on fibers and semiconductor waveguides. However, both these methods have their problems. In fiber devices, where longer interaction lengths are required, linear propagation of ultrashort pulses is difficult due to dispersion. And for the current optimum semiconductor device, namely,  $\text{Al}_x\text{Ga}_{1-x}\text{As}$  operating at near half the band edge, the large pulse intensity required to produce the required index change induces two-photon absorption that leads to additional carriers and, inevitably, unwanted attenuation of the propagating pulse.

In this paper we introduce plasma heating results based on the two-dimensional (2D), anisotropic semiconductor-Bloch equations (SBE's) for the SOA in the presence of an intense half-cycle 1 THz pulse. The heated carrier distributions are then utilized to calculate the THz-pulse-induced change in refractive index and gain profile. Since the e-h plasma is heated using intraband transitions, we circumvent the usual complications due to an overall change in density, and the nonlinear recovery is governed mainly by the carrier-LO-phonon interactions (typically 5–10 ps for a complete recov-

ery). This procedure implies very impressive, THz and sub-THz switching and recovery rates, respectively.

The dynamics of charged carriers (electrons and holes) in a semiconductor under the action of an external field has been of fascinating interest for many years. One classic example that was predicted more than four decades ago is the Franz-Keldysh effect,<sup>5</sup> i.e., the application of a static electric field in a periodic solid induces absorption below the band edge and oscillatory behavior of the absorption above. In superlattices, various effects including Zenner tunneling,<sup>6</sup> collapse of the miniband,<sup>7</sup> dynamic localization,<sup>8</sup> and more recently, reflection of THz radiation,<sup>9</sup> have been investigated. With the advent of free-electron lasers as well as solid-state THz sources,<sup>10</sup> the interplay between various elementary and collective intraband (THz) excitations and the interband optical properties has been receiving renewed attention from both the theoretical<sup>11</sup> and experimental<sup>12</sup> viewpoints. Moreover, two-color radiation methods (THz and NIR) applied to mesoscopic semiconductors<sup>13</sup> have been developed. Being relevant in the operation of high-speed electronic and optoelectronic devices such as photodetectors, modulators, and switches, the investigation of interplaying THz and optical fields is also of industrial and military interest.

Experimentally it is well established that under the influence of intense THz fields, the effects of electron and hole transport can be considerable. In the high density regime, nonlinear transport experiments reported in Ref. 14 were successfully explained by carrying out an effective temperature theory that characterized the plasma temperature as a function of the THz field parameters.<sup>15</sup> In the present paper we investigate carrier heating in a SOA by injecting an intense half-cycle THz pulse. Even for carrier densities as high as those in SOA's we will show that a THz pulse can heat the carriers substantially such that the dynamical modification of both the gain and refractive index can form the basis of a very efficient switch. In addition these effects are of fundamental interest since they provide a window on the interaction of dense semiconductor plasmas with strong non-stationary electric fields, and provide a link between transport and optical phenomena.

We begin by calculating the time-dependent plasma temperature of the carriers due to the application of a THz field. In the following theoretical treatment, we assume a two-band quantum well (QW) where each e-h state with relative wave

number  $\mathbf{k}$  contributes to the total carrier density  $N = 2A^{-1} \sum_{\mathbf{k}} n_{\mathbf{k}}^{e/h}$ . Here,  $n_{\mathbf{k}}^{e/h}$  is the electron or hole carrier distribution and the factor of 2 accounts for the spin summation;  $A$  is the normalization area. Since there is no optical field yet, we only have to solve for the carriers, and the appropriate dynamical charge-carrier distributions—derived from the SBE's—are simply

$$\left( \frac{\partial}{\partial t} + \mathbf{F}_{\text{THz}}(t) \cdot \nabla_{\mathbf{k}} \right) n_{\mathbf{k}}^e = \frac{\partial n_{\mathbf{k}}^e}{\partial t} \Big|_{\text{cc}}, \quad (1)$$

$$\left( \frac{\partial}{\partial t} + \mathbf{F}_{\text{THz}}(t) \cdot \nabla_{\mathbf{k}} \right) n_{-\mathbf{k}}^h = \frac{\partial n_{-\mathbf{k}}^h}{\partial t} \Big|_{\text{cc}}, \quad (2)$$

which is solved with the condition that  $n_{\mathbf{k}}^a(t=-\infty)$  ( $a = e, h$ ) are the initial isotropic Fermi-Dirac carrier distributions at room temperature ( $T = 300$  K). We assume that the initial incoherent carrier density is  $1 \times 10^{12} \text{ cm}^{-2}$ . Because the high density regime in amplifiers is considered, Coulomb correlations (cc) between the carriers must be taken into account [ $\dot{n}_{\mathbf{k}}|_{\text{cc}}$  contribution in Eq. (1)]. It has been reported that, for large plasma densities in rapidly varying THz fields, carrier-carrier scattering thermalizes the distributions so rapidly that the modified distribution functions can be characterized by an effective carrier temperature (quasiequilibrium temperature).<sup>14,15</sup> Hence, for the following calculations we employ a relaxation-time approximation (RTA) for the Coulomb correlations. The RTA can be derived assuming a simple exponential decay of a small deviation from a quasiequilibrium carrier distribution—with the conditions that the total momentum and carrier density are conserved quantities. Subsequently, the intraband scattering for the carrier distribution functions is given by  $\dot{n}_{\mathbf{k}}^a|_{\text{cc}} = -\gamma_a^{\text{cc}} [n_{\mathbf{k}}^a - F_{\mathbf{k}}(\mu^a, T_{\text{pl}})]$ , where  $F$  denotes the Fermi functions with chemical potentials  $\mu^a$  and plasma temperature  $T_{\text{pl}}$  ( $a = e, h$ ). The relaxation rate  $\gamma_a^{\text{cc}}$  is  $\mathbf{k}$ -independent as a consequence of carrier conservation. We assume  $\gamma_a^{\text{cc}} = 70$  fs for both the electrons and holes. By employing the intraband RTA, the plasma temperature has to be computed dynamically because carrier-carrier scattering leaves the total kinetic energy of the carrier system unchanged.

The influence of the THz pulse is described by the partial derivatives with respect to the carrier quasimomentum that appears on the left-hand side of Eqs. (1) and (2). This term leads to a shift of the distribution functions in  $\mathbf{k}$  space according to the acceleration theorem  $\partial_t \mathbf{k} = e \mathbf{F}_{\text{THz}}$ . Thus our theoretical model arrives at the level of the anisotropic 2D-SBE's for the carriers that fully incorporate the acceleration of the electrons and holes due to an applied field. For the QW we choose material parameters close to  $\text{In}_x\text{Ga}_{1-x}\text{As}$  QW's: electron/hole mass ratio, 4/6; 1s excitonic binding energy,  $E_x = 12$  meV; three-dimensional Bohr radius,  $a_0 = 15$  nm; and interband dipole moment  $d_{cv} = 0.4 e \text{ nm}$  ( $e$  is the electron charge). For the applied THz field we employ  $\mathbf{F}_{\text{THz}}(t) = \hat{\mathbf{n}}_x F_0 \sin(2\pi \nu_{\text{THz}} t)$ , with  $F_0 = 10$  kV/cm the magnitude of the field,  $\hat{\mathbf{n}}_x$  a unit vector in the  $x$  direction (in the QW plane), and  $\nu_{\text{THz}} = 1$  THz ( $\hbar \omega_{\text{THz}} \approx 4$  meV). For the THz field, we only consider a half cycle.

As the electrons and holes are driven apart by the THz field a space-charge field is created. However, we estimate

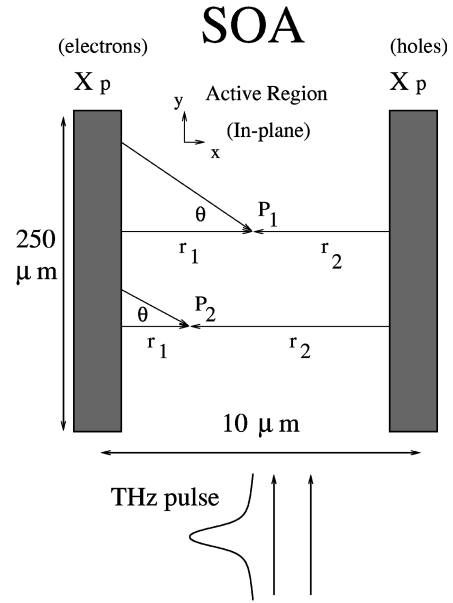


FIG. 1. Schematic of the proposed experiment.  $X_p$  corresponds to the maximum distance that the electrons and holes can be driven apart by the THz field. The labeled points,  $P_1$  and  $P_2$ , are chosen for our simple screening analysis.

that for our studies, for all our intents and purposes, the screening field is small. The magnitude of the screening field can be calculated using a simple model in which the positive and negative line charges lie at the extremes of the SOA structure. In Fig. 1 a schematic of our proposed experiment is shown. The length of the SOA is taken to be  $250 \mu\text{m}$ , while the width is  $10 \mu\text{m}$ . Our SOA structure is chosen to be close to that on which experiments have been undertaken.<sup>3</sup> We assume light propagation in the plane of the QW. Since realistic laser geometries employ several QW's, we assume that different QW's can be treated as independent of each other.  $X_p$  is the maximum distance that the electrons and holes can be pulled apart. We calculate that in the absence of scattering,  $X_p = 13.5$  nm but in reality it will be substantially less. In the spirit of Gauss' theorem, we proceed by estimating the screening field at typical points  $P_1$  and  $P_2$  from  $E_s = \int_{-\pi/2}^{\pi/2} d\theta \zeta / \kappa \epsilon_0 [r_1 + r_2] \cos(\theta)$ , where  $\kappa$ ,  $\epsilon_0$ , and  $\zeta$  are the dielectric constant, permittivity of free space, and the line-charge density, respectively;  $r_1$  and  $r_2$  are the perpendicular distances from the SOA extremes (electron and hole line charges). A constraint for the above analysis is that the number of quantum wells should not be too many and/or that the barrier lengths (between QW's) should be sufficiently large, since for  $N$  closely separated QW's this may increase the screening field by a factor of  $N$ . In practice, this is not a serious burden as usually only about 2–4 QW's are used which are adequately separated. Employing the above value of  $X_p$  and  $\kappa = 13.7$ , the screening fields at  $P_1$  and  $P_2$  are respectively calculated to be  $0.4$  kV/cm and  $0.7$  kV/cm. Given that these are significantly smaller than  $F_0$  as well as conservative upper bounds for the screening fields, we push on with our investigation neglecting space-charge screening.

In Fig. 2(a) we depict the generalized plasma temperature (solid curve) extracted from the kinetic energy of the non-equilibrium distribution functions. As can be recognized, the plasma temperature heats substantially as the THz field pulls

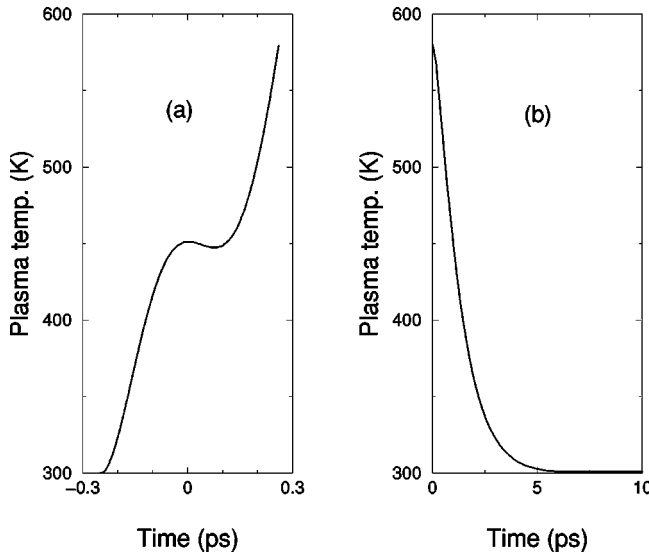


FIG. 2. (a) Generalized plasma temperature, extracted numerically from the kinetic energy of the nonequilibrium distribution functions (induced by the application of a 1 THz half-cycle pulse). The carrier density is  $1 \times 10^{12} \text{ cm}^{-2}$ . (b) Plasma temperature (same for the electrons and holes) of the relaxing carrier distributions (after the THz pulse has gone) due to e-h interactions with the LO phonons.

the electrons and holes apart. After the THz field reaches its maximum, any carriers that are not in quasiequilibrium are pulled back together again and the temperature reduces slightly. The fact that this reduction is slight demonstrates the validity of our RTA assumption, since the nonequilibrium distribution functions are not too far from circularly symmetric Fermi functions due to fast e-h carrier-carrier scattering. Since kinetic energy is continually being added to the system, the carriers heat up again, eventually reaching a temperature of approximately 580 K after the half-cycle THz pulse. Moreover, the plasma heating is much faster than can be achieved via current switching, which is typically 10 GHz at best. Note that if the carrier-carrier intraband lifetimes were much longer, then the carrier temperature would oscillate from a minimum to a maximum twice during a full cycle.<sup>15</sup> By applying the classical equations of motion for a free electron subject to the appropriate initial conditions,  $\xi(t) = -\xi_0[\cos(\omega_{\text{THz}}t) - 1]$  describes the motion of an electron in the absence of scattering. Thus, after  $\omega_{\text{THz}}t$  becomes greater than  $\pi/4$  (a quarter period) the motion of the electron will be *dragged* back to its original position and forced in the opposite direction after a THz half cycle. For the low-density regime, in the presence of an optical pulse, this is manifested in interfering and beating, e-h relative motion wavepackets.<sup>16</sup> In Fig. 2(b), we show the generalized plasma temperature after the THz pulse, whereby the heated distribution relaxes back to the lattice temperature. A carrier-LO-phonon lifetime of 1 ps is chosen in agreement with experiments (see, for example, Ref. 2). A complete recovery of the nonlinearity occurs within 5–10 ps. Our theory does not account for possible hot phonon effects that may be important on much longer timescales for the SOA. Nevertheless, we expect thermal effects to be suppressed in our case because the specific heat of the phonon bath is very small. The actual amount of lattice heating is strongly dependent on device design.<sup>17</sup>

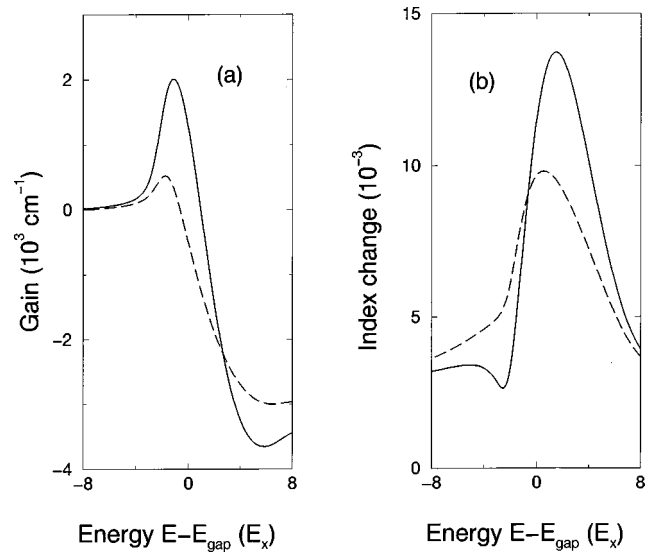


FIG. 3. (a) Material gain spectrum of the initial and heated carrier distributions [cf. Fig. 2(a)]. The energy is labeled in units of the QW 1s excitonic binding energy. (b) Change in modal refractive index of the initial and heated carrier distributions. A waveguide confinement factor of  $\Gamma = 0.2$  has been assumed.

Next we calculate the interband (optical) gain and refractive index profiles before and after the application of the THz pulse. In our quantitative analysis we include correlation effects beyond the Hartree-Fock level that describe dephasing and intraband Coulomb correlations in second Born approximation. We include both diagonal and nondiagonal dephasing and employ the full SBE's,<sup>18</sup> including a renormalized energy dispersion for a parabolic two-band semiconductor [band-gap renormalization (BGR)] and the generalized Rabi frequency (Coulombic enhancement). The Coulomb potential is treated in a quasistatic screening model. The carrier-carrier scattering is calculated from the e-h Boltzmann equation,  $\dot{n}_{\mathbf{k}|cc}^a = \Gamma_{\text{in},\mathbf{k}}^a(\mathbf{k},n)[1 - n_{\mathbf{k}}^a] - \Gamma_{\text{out},\mathbf{k}}^a(\mathbf{k},n)n_{\mathbf{k}}^a$ , where  $\Gamma_{\text{in},\mathbf{k}}^a$  and  $\Gamma_{\text{out},\mathbf{k}}^a$  ( $a = e, h$ ) are the usual expressions for *in* and *out* scattering. Similarly, the polarization scattering<sup>19</sup>  $\dot{P}_{\mathbf{k}|cc} = -\Gamma_{\text{D}}^{\text{p}}(\mathbf{k},n)P_{\mathbf{k}} + \sum_{\mathbf{q}}\Gamma_{\text{ND}}^{\text{p}}(\mathbf{k},\mathbf{q},n)P_{|\mathbf{k}+\mathbf{q}|}$ , where the total diagonal dephasing rate  $\Gamma_{\text{D}}^{\text{p}}$  is one-half times the sum over all distribution scattering rates and hence accounts for loss of polarization. The additional scattering rate describes the rate of polarization transfer (nondiagonal dephasing) between the states  $\mathbf{k}$  and  $\mathbf{q}$ . The macroscopic polarization is obtained from  $P = 2A^{-1}\sum_{\mathbf{k}}P_{\mathbf{k}}$ , which is used to obtain the SOA optical susceptibility. The prediction of gain spectra using the microscopic theory employed here is very accurate and accounts self-consistently for highly non-Lorentzian line shapes; for a comparison with the experiments compare, for instance, Refs. 19.

In Fig. 3(a) we plot the material gain spectrum versus the detuning of the electromagnetic energy  $\hbar\omega$  with respect to the band edge for the initial (solid curve) and heated (dashed curve) carrier distributions. As usual, the density-dependent part of the BGR generates gain below the band edge. After the THz field has interacted with the SOA, the peak gain is reduced dramatically without any net carrier-density change. The transparency point (TP) has also shifted accordingly. As the plasma heats, carriers move from lower momentum states

to higher ones and less carriers are available for stimulated emission. We have verified numerically that one can control the position of the heated TP simply by changing the magnitude of the THz pulse (assuming that it is not too large as to completely saturate the gain). On longer time scales [see Fig. 2(b)], the plasma cools and gain regeneration will occur as the carriers once again become available for stimulated emission.

How does the THz pulse affect the SOA refractive index? Figure 3(b) demonstrates that modal refractive index changes of the order of 0.002 can easily be created; this calculation employs a typical wave-guide confinement factor,  $\Gamma=0.2$ . Assuming then that one wishes to induce a  $\pi$  phase shift: a propagation length of only  $\Delta z^\pi=215 \mu\text{m}$  ( $\pi/k\Delta n$ ) is required.<sup>20</sup> In real laser structures this propagation length will scale inversely with  $\Gamma$  and is highly material-dependent ( $\Delta z^\pi \propto 1/d_{cv}^2 \Gamma$ ). With regards to optical switching it is sometimes convenient to define specific device figures-of-merit, for example in a Fabry-Pérot configuration:<sup>21</sup>  $F=5|\Delta n|k/\pi\alpha > 1$ , where  $\alpha$  is the absorption coefficient. In our case, by operating near the heated transparency point,  $F$  can be extremely large because  $\alpha$  is close to zero. For very short pulses though, one must be careful with propagating exactly at the e-h chemical potential as polariton-type dispersive beating may occur.<sup>22</sup> Another commonly quoted figure-of-merit for switching via resonant optical nonlinearities (which usually have the problem of a slow, ns decay) is  $F=|\Delta n|/\alpha\tau > 1$ , where  $\tau$  is the recovery time. Again, this is

easy to satisfy here both above and below the band edge since the recovery times are sufficiently fast and the change in refractive index is huge in comparison to those that can be generated via excitation near half the band edge. Consequently, from the point of view of ultrafast optical switching, the figures-of-merit suggest that our proposed scheme is very attractive indeed.

In conclusion, we have theoretically investigated e-h plasma temperature changes in a SOA using an intense half-cycle THz pulse. A significant ultrafast heating of the plasma was demonstrated without any additional carrier generation. The subsequent changes of the SOA gain and refractive index were calculated using a self-consistent microscopic theory. We have specialized our analysis to the lower density gain regime, where the differences are more dramatic and the space-charge screening field can be neglected. Our results imply that THz pulses may be used in conjunction with the SOA to form the basis of a very efficient ultrahigh-speed optical switch using either gain modulation or index modulation. Future studies to investigate laser switch-off behavior by solving the full dynamical laser equations and Boltzmann calculations of anisotropic carrier-carrier scattering are under way.

We thank T. B. Norris and C. Z. Ning for stimulating discussions. This work was supported by the National Science Foundation under Grant No. DMR9705403 and by the Office of Naval Research.

\*FAX: +1 509 335-7816. Electronic address: shughes@wsu.edu

<sup>1</sup>See, for example, theory: A. Knorr *et al.*, *Opt. Lett.* **18**, 1538 (1993); F. Jahnke and S. W. Koch, *Appl. Phys. Lett.* **67**, 2278 (1995); experiment: C. T. Hultgren *et al.*, *ibid.* **61**, 2767 (1992); J. Mørk *et al.*, *ibid.* **64**, 2206 (1994).

<sup>2</sup>S. G. Hense and M. Wegener, *Phys. Rev. B* **55**, 9255 (1997); M. Elsässer *et al.*, *Appl. Phys. Lett.* **70**, 853 (1997).

<sup>3</sup>See, for example, C. T. Hultgren and E. P. Ippen, *Appl. Phys. Lett.* **59**, 635 (1991); K. L. Hall *et al.*, *ibid.* **62**, 1320 (1993).

<sup>4</sup>C. N. Ironside, *Contemp. Phys.* **34**, 1 (1993).  
<sup>5</sup>W. Franz, *Z. Naturforsch. Teil A* **13**, 484 (1958); L. V. Keldysh, *Zh. Eksp. Teor. Fiz.* **34**, 1138 (1958) [*Sov. Phys. JETP* **34**, 788 (1958)].

<sup>6</sup>F. Bloch, *Z. Phys.* **52**, 555 (1929).

<sup>7</sup>M. Holthaus, *Phys. Rev. Lett.* **69**, 351 (1992).

<sup>8</sup>T. Meier *et al.*, *Phys. Rev. Lett.* **73**, 902 (1994).

<sup>9</sup>A. W. Ghosh *et al.*, *Phys. Rev. Lett.* **79**, 3494 (1997).

<sup>10</sup>See, for example, P. C. M. Planken *et al.*, *Phys. Rev. Lett.* **69**, 3800 (1992); S. L. Chuang *et al.*, *ibid.* **68**, 102 (1992); D. S. Citrin, *Opt. Express* **4**, 376 (1997).

<sup>11</sup>See, for example, A. P. Jauho and K. Johnsen, *Phys. Rev. Lett.* **24**, 4576 (1996).

<sup>12</sup>See, for example, K. B. Nordstrom *et al.*, *Phys. Status Solidi B* **204**, 52 (1997).

<sup>13</sup>J. Kono *et al.*, *Phys. Rev. Lett.* **79**, 1758 (1997).

<sup>14</sup>N. G. Asmar *et al.*, *Phys. Rev. B* **51**, 18 041 (1995).

<sup>15</sup>X. L. Lei *et al.*, *Phys. Rev. B* **56**, 12 120 (1997).

<sup>16</sup>S. Hughes and D. S. Citrin (unpublished).

<sup>17</sup>See, for example, C. Z. Ning *et al.*, *J. Opt. Soc. Am. B* **12**, 1993 (1995).

<sup>18</sup>For a recent review that also includes nondiagonal dephasing, see A. Knorr *et al.*, *J. Chem. Phys.* **210**, 27 (1996), special issue, and references therein.

<sup>19</sup>S. Hughes *et al.*, *Solid State Commun.* **100**, 555 (1996); W. W. Chow *et al.*, *Appl. Phys. Lett.* **71**, 157 (1997); S. Hughes, *Opt. Lett.* **24**, 948 (1998).

<sup>20</sup>For this length estimation we have employed a waveguide confinement factor typical of a few QW's (0.2). For a single QW, the required propagation length may be  $\sim 5$  times greater depending on the exact geometry of the structure.

<sup>21</sup>See, for example, D. C. Hutchings *et al.*, *J. Opt. Soc. Am. B* **8**, 618 (1991).

<sup>22</sup>Theory: S. Hughes *et al.*, *Opt. Lett.* **21**, 1052 (1996); experiment: Y.-H. Kao *et al.*, *Appl. Phys. Lett.* **69**, 4227 (1996).